Biochimica et Biophysica Acta 1840 (2014) 3106–3114

Contents lists available at ScienceDirect

Biochimica et Biophysica Acta

journal homepage: www.elsevier.com/locate/bbagen

A ^{1}H NMR study of the specificity of α-L-arabinofuranosidases on natural and unnatural substrates

Vinciane Borsenberger [a,b,c], Emmie Dornez [d], Marie-Laure Desrousseaux [a,b,c], Stéphane Massou [a,b,c], Maija Tenkanen [e], Christophe M. Courtin [d], Claire Dumon [a,b,c], Michael J. O'Donohue [a,b,c], Régis Fauré [a,b,c,*]

[a] Université de Toulouse; INSA, UPS, INP; LISBP, 135 Avenue de Rangueil, F-31077 Toulouse, France
[b] INRA, UMR792 Ingénierie des Systèmes Biologiques et des Procédés, F-31400 Toulouse, France
[c] CNRS, UMR5504, F-31400 Toulouse, France
[d] Laboratory of Food Chemistry and Biochemistry, KU Leuven, Kasteelpark Arenberg 20 bus 2463, B-3001 Leuven, Belgium
[e] Department of Food and Environmental Sciences, Faculty of Agriculture and Forestry, University of Helsinki, P.O. Box 27, FI-00014 Helsinki, Finland

ARTICLE INFO

Article history:
Received 20 December 2013
Received in revised form 17 June 2014
Accepted 1 July 2014
Available online 10 July 2014

Keywords:
Arabinoxylan arabinofuranohydrolases
Di-arabinofuranosylated substrates
Enzymatic hydrolysis
Specificity
Screening
NMR

ABSTRACT

Background: The detailed characterization of arabinoxylan-active enzymes, such as double-substituted xylan arabinofuranosidase activity, is still a challenging topic. Ad hoc chromogenic substrates are useful tools and can reveal subtle differences in enzymatic behavior. In this study, enzyme selectivity on natural substrates has been compared with enzyme selectivity towards aryl-glycosides. This has proven to be a suitable approach to understand how artificial substrates can be used to characterize arabinoxylan-active α-L-arabinofuranosidases (Abfs).
Methods: Real-time NMR using a range of artificial chromogenic, synthetic pseudo-natural and natural substrates was employed to determine the hydrolytic abilities and specificity of different Abfs.
Results: The way in which synthetic di-arabinofuranosylated substrates are hydrolyzed by Abfs mirrors the behavior of enzymes on natural arabinoxylo-oligosaccharide (AXOS). Family GH43 Abfs that are strictly specific for mono-substituted D-xylosyl moieties (AXH-m) do not hydrolyze synthetic di-arabinofuranosylated substrates, while those specific for di-substituted moieties (AXH-d) remove a single L-arabinofuranosyl (L-Ara*f*) group. GH51 Abfs, which are supposedly AXH-m enzymes, can release L-Ara*f* from disubstituted D-xylosyl moieties, when these are non-reducing terminal groups.
Conclusions and general significance: The present study reveals that although the activity of Abfs on artificial substrates can be quite different from that displayed on natural substrates, enzyme specificity is well conserved. This implies that carefully chosen artificial substrates bearing di-arabinofuranosyl D-xylosyl moieties are convenient tools to probe selectivity in new Abfs. Moreover, this study has further clarified the relative promiscuity of GH51 Abfs, which can apparently hydrolyze terminal disubstitutions in AXOS, albeit less efficiently than mono-substituted motifs.

1. Background

α-L-Arabinofuranosidases (Abfs — EC 3.2.1.55) involved in the deconstruction of arabinoxylans (AX) and arabinoxylo-oligosaccharides (AXOS) are generally considered to be *exo*-enzymes that remove non-reducing L-arabinofuranosyl (L-Ara*f*) residues from xylan and xylo-oligosaccharidic backbone, being able to cleave α-1,2 and/or α-1,3 linkages [1,2]. Currently AX-specific Abfs (i.e. arabinoxylan arabinofuranohydrolases, designated AXH) are found in families GH2, 3, 43, 51, 54 and 62 within the CAZy database [3] and are named according to their hydrolytic specificities (Fig. 1). Abfs that release L-Ara*f* units from mono-substituted main-chain D-xylopyranosyl (D-Xyl*p*) motifs are termed AXH-m, while those that release single L-Ara*f* residues from double-substituted main-chain D-Xyl*p* motifs are termed AXH-d. Moreover, when the exact bond specificity is known, this nomenclature can be completed by a numeral. Hence, AXH-d3 is an Abf that cleaves α-1,3 bonds that link L-Ara*f* unit to a doubly-substituted D-Xyl*p* residue.

AXH-m are the most common type of Abf and are widespread in family GH51. Mostly, these enzymes have been reported to possess

Abbreviations: Abfs, α-L-arabinofuranosidases; AX, arabinoxylans; AXH, arabinoxylan arabinofuranohydrolase; AXH-d3, double-substituted xylan α-1,3-L-arabinofuranosidase; AXH-m, mono-substituted xylan α-L-arabinofuranosidase; AXOS, arabinoxylo-oligosaccharides; Bz, benzoyl; Bn, benzyl; D-Xylp, D-xylopyranosyl; GH, glycoside hydrolase; L-Ara, L-arabinose; L-Ara*f*, L-arabinofuranosyl; 4NTC, 4-nitrochatecol; pNP, *para*-nitrophenol; pNPA, *para*-nitrophenyl α-L-arabinofuranoside; SA, specific activity; *Tx*Abf, α-L-arabinofuranosidase from *Thermobacillus xylanilyticus*

* Corresponding author at: Laboratoire d'Ingénierie des Systèmes Biologiques et des Procédés, 135 Avenue de Rangueil, 31077 Toulouse cedex 4, France. Tel.: +33 5 6155 9488; fax: +33 5 6155 9400.
E-mail address: regis.faure@insa-toulouse.fr (R. Fauré).

http://dx.doi.org/10.1016/j.bbagen.2014.07.001
0304-4165/

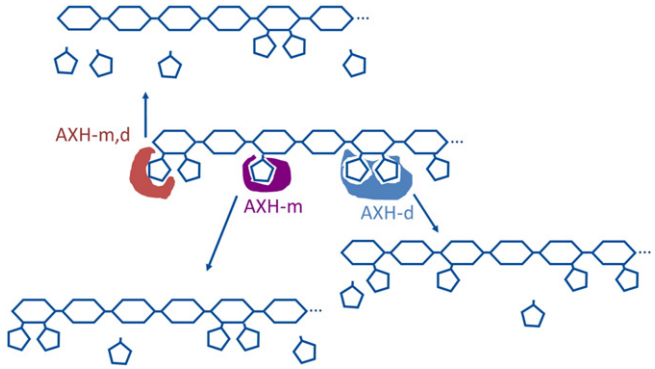

Fig. 1. Subclasses of arabinoxylan-active Abfs (AXH) according to substrate specificities (hexagons: D-Xyl*p* units; pentagons: L-Ara*f* units).

the ability to hydrolyze simple chromogenic substrates, such as *para*-nitrophenyl α-L-arabinofuranoside (pNPA) and to show fairly strict specificity for mono-substituted D-Xyl*p* in AX and AXOS, observations that are consistent with structural data, which in the case of GH51 Abfs reveal that the active site is characterized by a deep −1 subsite that tightly accommodates a single L-Ara*f* unit [4,5]. In contrast, the GH43 AXH-m specific AbfA from *Bifidobacterium adolescentis* (GenBank accession no BAF39204.1) [6] displays almost no activity on pNPA, while being able to hydrolyze mono-substituted 4-nitrocatechol (4NTC) homologues [7], suggesting that the enzyme needs to recognize both the L-Ara*f* unit and its adjacent hydroxyl group on the D-Xyl*p* residue.

So far, three enzymes have been reliably described as AXH-d [8–10], with all these belonging to family GH43. The rather singular specificity of these enzymes appears to be determined by their ability to recognize the L-Ara*f* unit vicinal to the departing sugar moiety. In a recent study of *Hi*AXH-d3 from *Humicolens insolens* (CAL81199.1), it was reported that this enzyme possesses a deep active site pocket (subsite −1) that accommodates a 1,3-linked L-Ara*f* and an adjacent shallow binding subsite that accommodates the vicinal 1,2-linked L-Ara*f* [11]. Unlike the aforementioned GH43 AXH-d enzymes, which display tight substrate specificity, some GH51 enzymes appear to be more promiscuous [6,12–14], being principally AXH-m, but displaying some activity on di-arabinofuranosylated D-Xyl*p* moieties (denoted AXH-m,d). For instance, it has been reported that Abf51A from *Cellvibrio japonicus* (ACE86344.1) displays a weak ability to release L-Ara from double-substituted D-Xyl*p* moieties, although its activity on mono-substituted D-Xyl*p* is 1000 times higher [12], and AXAH-1 from *Hordeum vulgare* (AAK21879.1) [13,14] was shown to be able to hydrolyse disubstituted D-Xyl*p* moieties when these form the non-reducing terminal sugar in AXOS.

Overall, the comparison and classification of Abfs is not straightforward, particularly when using oversimplified synthetic substrates (i.e. mono-glycosides linked directly to aglycon groups, such as pNP), or complex substrates (e.g. AX) combined with informationally-poor methods, such as the measurement of the release of reducing sugars, neither of which allow the study of selectivity. Therefore, to address this challenge, we have devised a strategy that combines the use of a set of substrates displaying different structural features and ^{1}H NMR analysis [6,10,13]. Together, these provide the means to reveal the fine details of Abf activity, in particular regioselectivity. To demonstrate the power of this approach, we have addressed the question of how the presence of a doubly-linked L-Ara*f* motif in substrates affects the activity of different Abfs from GH43 and GH51 families.

2. Material and methods

2.1. General reagents and methods

Chemicals were purchased from either Sigma-Aldrich or ACROS and used as received, without further purification. Sodium acetate[D_3] and acetic acid[D_4] used for the preparation of deuterated buffer were purchased from Euriso-top (Saint-Aubin, France). DCM was distilled from P_2O_5, prior to use. The evolution of synthetic reactions was monitored using analytical thin-layer chromatography, employing silica gel 60 F254 precoated plates (E. Merck). Spots were visualized using ultraviolet light (254 nm) and then by soaking in a 10% w/v orcinol solution containing a mixture of sulfuric acid/ethanol/water (3:72.5:22.5 v/v/v) followed by charring. Purification of reactions products was achieved using silica gel Si 60 (40–63 μm) using a bench column, operating with the indicated eluent, or using a Reveleris® flash chromatography automated system (Grace, Epernon, France) equipped with prepacked cartridges (Grace). Yields refer to chromatographically pure compounds. NMR spectra were recorded at 298 K on a Bruker Avance II 500 spectrometer or on a Bruker Avance 600 spectrometer equipped with a TCI cryoprobe. Coupling constants (*J*) are reported in Hz, chemical shifts (δ) are given in ppm. Multiplicities are reported as follows: s = singlet, d = doublet, t = triplet, m = multiplet, br s = broad singlet, dd = doublet of doublets, td = triplet of doublets. Analysis and assignments were made using 1D (^{1}H, ^{13}C and J-modulated spin-echo (Jmod)) and 2D (COrrelated SpectroscopY (COSY) and Heteronuclear Single Quantum Coherence (HSQC)) spectra. High-resolution mass spectra (HRMS) analyses were performed by the CRMPO (Centre régional de mesures physiques de l'Ouest, University of Rennes, France) in positive ionization mode (ES^+) on a Waters Q-Tof 2.

2.2. Artificial, pseudo-natural and natural substrates

Substrates **1** and **2** were synthesized as described in previous work [7,15].

Substrate **3** was synthesized in-house (Supplementary Fig. 2). First, to prepare benzyl 4-*O*-benzoyl-2,3-di-*O*-(2,3,5-tri-*O*-benzoyl-α-L-arabinofuranosyl)-β-D-xylopyranoside **7**, working under nitrogen, benzyl 4-*O*-benzoyl-β-D-xylopyranoside **5** (328 mg, 0.95 mmol, 1 eq.) [16] was partially dissolved in anhydrous DCM (25 mL) in a two-neck flask equipped with a pressure-equalizing dropping funnel. Using a syringe, $BF_3 \cdot Et_2O$ (60 μL, 0.49 mmol, 0.5 eq.) was added to the stirred yellow suspension. Next, trichloroacetimidate **6** (1.33 g, 2.19 mmol, 2.3 eq.) [17] was dissolved in anhydrous DCM (10 mL) in the presence of activated molecular sieves (4 Å), and was slowly transferred to the reaction mixture over 20 min via the dropping funnel. The funnel was rinsed with 10 mL of anhydrous DCM, which were further added to the reaction. The mixture was stirred at room temperature for 60 min, and then neutralized with triethylamine. After, the residue was transferred to a decanting funnel and water (50 mL) was added. After separation, the aqueous phase was extracted twice with DCM. The combined organic extracts were first washed with a saturated solution of $NaHCO_3$, then with a small amount of water, and finally with brine, before being dried ($MgSO_4$), filtered, and evaporated. The residue was purified by automated flash column chromatography, using a 20 to 40% gradient of EtOAc in petroleum ether, which provided compound **7** as a white solid (676 mg, 0.55 mmol, 56%). ^{1}H NMR (500 MHz, $CDCl_3$, 298 K) δ 8.07–8.05 (m, 2H), 7.95–7.91 (m, 6H), 7.90–7.88 (m, 2H), 7.75–7.74 (m, 2H), 7.69–7.67 (m, 2H), 7.61–7.56 (m, 2H), 7.49–7.39 (m, 9H), 7.32–7.29 (m, 2H), 7.23–7.14 (m, 13H), 5.80 (s, 1H), 5.79 (s, 1H), 5.53 (d, 1H, J = 0.6), 5.45 (d, 1H, J = 4.3), 5.44 (d, 1H, J = 0.5), 5.41 (d, 1H, J = 4.0), 5.32–5.27 (m, 1H), 4.85 (d, 1H, J = 11.0), 4.67 (d, 1H, J = 7.0), 4.56–4.54 (m, 1H), 4.52 (dd, 1H, J = 11.9, 3.2), 4.43–4.32 (m, 5H), 4.27 (dd, 1H, J = 12.2, 5.5), 4.24 (dd, 1H, J = 11.7, 4.4), 4.10 (dd, 1H, J = 9.7, 7.0), 3.53 (dd, 1H, J = 12.2, 7.7); ^{13}C NMR (126 MHz, $CDCl_3$, 298 K) δ 166.2, 166.0, 165.5, 165.5, 165.5, 165.4, 165.3, 136.7, 133.6, 133.5, 133.5, 133.1, 133.0, 133.0, 132.9, 132.8, 129.9, 129.9, 129.8, 129.8, 129.7, 129.7, 129.6, 129.5, 129.4, 129.3, 129.1, 128.9, 128.9, 128.5, 128.4, 128.4, 128.4, 128.2, 128.2, 128.2, 128.2, 128.1, 106.5, 106.0, 101.6, 81.9, 81.8, 81.8, 81.7, 77.9, 77.7, 77.3, 77.1, 71.7, 71.2, 63.4, 63.4, 63.2. Next, to synthesize benzyl 2,3-di-*O*-α-L-arabinofuranosyl-β-D-xylopyranoside **3**, working under nitrogen, **7**

(254 mg, 0.21 mmol, 1 eq.) was dissolved in a mixture of anhydrous methanol and DCM (2:1 v/v, 21 mL) at 0 °C. Then, a solution of MeONa in methanol (1 M, 0.2 mL, 0.2 mmol, 1 eq.) was added dropwise. The reaction mixture was stirred at room temperature for 5 h, neutralized with Amberlite IR-120 (H^+), and filtered. The filtrates were concentrated under reduced pressure. Next, the residue was further purified using an automated flash column chromatography system equipped with a C_{18} silica column (12 g) and operating in a 15 to 25% gradient of acetonitrile in water. Product-containing fractions were concentrated, filtered (45 μm filter), and lyophilized, affording **3** (80 mg, 0.16 mmol, 77%) as a white powder. ^{1}H NMR (500 MHz, D_2O, 298 K) δ 7.49–7.39 (m, 5H), 5.24 (d, 1H, J = 1.5), 5.18 (d, 1H, J = 1.2), 4.88 (d, 1H, J = 11.1), 4.66 (d, 1H, J = 11.1), 4.64 (d, 1H, J = 7.8), 4.19 (td, 1H, J = 5.9, 4.2), 4.16 (dd, 1H, J = 3.4, 1.7), 4.10 (dd, 1H, J = 2.6, 1.3), 4.02 (dd, 1H, J = 11.8, 4.9), 3.96 (dd, 1H, J = 6.0, 3.2), 3.94–3.90 (m, 2H), 3.81 (dd, 1H, J = 12.3, 3.4), 3.74–3.67 (m, 3H), 3.53 (dd, 1H, J = 8.8, 7.6), 3.48 (dd, 1H, J = 12.6, 3.8), 3.44 (dd, 1H, J = 12.6, 3.2), 3.37 (dd, 1H, J = 11.8, 9.7); ^{13}C NMR (126 MHz, D_2O, 298 K) δ 136.5, 129.0, 128.7, 128.5, 108.5, 108.5, 101.0, 83.9, 83.8, 82.1, 81.4, 81.1, 77.9, 76.5, 76.4, 71.9, 68.0, 64.7, 61.2, 60.2; HRMS (ESI): m/z: calculated for $C_{22}H_{32}O_{13}Na$ ($[M + Na]^+$): 527.17406, found 527.1741 (0 ppm).

The AXOS, $A^{2+3}XX$ **4** [18], was isolated as previously described [19].

2.3. Enzymes

AbfA, AbfB and *Ba*AXH-d3 (BAF39204.1, BAF40305.1 and AAO67499.1), all from *B. adolescentis*, and *Tx*Abf from *Thermobacillus xylanilyticus* (CAA76421.2), are recombinant enzymes whose production has been previously described [6,10,20]. Briefly, these are produced in *Escherichia coli* as recombinant proteins (cloning coding sequences into pEXP5-CT/TOPO or pET expression vectors), each C-terminally fused to a His_6 tag, which facilitates purification from filtered lysate using immobilized metal affinity chromatographic technology (HiTrap HP 1 mL columns for the bifidobacterial enzymes and Clontech CellThru 10 mL disposable column containing TALON® Metal Affinity Resin for *Tx*Abf). After purification, the concentration of protein solutions was determined spectrophotometrically at 280 nm, using relevant extinction coefficients (96720, 115850, 158140 and 115320 $M^{-1}\cdot cm^{-1}$ for *Ba*AXH-d3, AbfA, AbfB and *Tx*Abf, respectively) and enzyme purity (>95%) was verified using SDS-PAGE, before storing enzymes in appropriate buffers (25 mM citrate pH 6.0 for bifidobacterial enzymes and 20 mM Tris–HCl pH 8.0 for *Tx*Abf) at 4 °C until use.

2.4. Real time ^{1}H NMR monitoring of enzyme reactions

Enzyme-mediated hydrolysis of **1**, **2**, and **3** was monitored by ^{1}H NMR, performing reactions in standard 5 mm NMR tubes, containing 500 μL of deuterated sodium acetate buffer (20 mM), pD 5.87, containing 5 mM substrate. Measurement of pD was performed using a glass pH electrode, applying the following relationship $pD = pH_{electrode} + 0.41$ [21]. Prior to the reactions, the enzyme was diluted by 10-fold in D_2O (99.90%), followed by concentration using an Amicon® Ultra filter (regenerated cellulose 10 kDa, Millipore) system, this operation being performed twice. Next, hydrolyses were initiated by the addition of an aliquot of the deuterated enzyme solution and reactions were performed at the optimum temperature of the studied enzyme (30 °C or 303 K for AbfB and *Ba*AXH-d3, 50 °C or 323 K for AbfA and 60 °C or 333 K for *Tx*Abf). Control experiments that did not contain enzyme were conducted in parallel, in order to monitor the spontaneous hydrolysis of substrates. After 24 h, a small amount of substrate **2** spontaneously hydrolyzed into **2a** and **2b** — 5% at 50 °C and 15% at 60 °C. Substrates **1** and **3** remained stable over 24 h within the considered temperature range. Overall, the stability of the substrates was judged sufficient, since the only sensitive experiment (*Tx*Abf with substrate **2**) did not exceed 200 min. The enzyme-mediated hydrolysis of **4** (2 mM) was performed in 3 mm NMR tubes at 600 MHz for improved sensitivity. In typical experiments, upon enzyme addition and mixing, the NMR tube was immediately transferred to the spectrometer, and after temperature stabilization, spectra consisting of an 8-scan accumulation were recorded continuously, thus providing the first spectrum 6 to 10 min after enzyme addition.^{1}H NMR scans were accumulated continuously over 1.45 min (8 scans with a repetition delay of 6 s) during 4 to 15 h, depending on the reaction. Each NMR spectrum was acquired using an excitation flip angle of 30° at a radiofrequency field of 29.7 kHz, and the residual water signal was pre-saturated during the repetition delay (with a radiofrequency field of 21 Hz). The following acquisition parameters were used: relaxation delay (5 s) and dummy scans (2).

2.5. Choice of significant protons

All spectral chemical shifts were calibrated by setting the acetate buffer peak at 1.92 ppm, because a separate control experiment demonstrated that this value is unaffected within the experimental temperature range (i.e. 303 to 333 K). Similarly, signals from substrates and products provided stable chemical shifts, within 0.01 ppm, from one series of experiments to another. The residual acetate peak was also utilized as a reference for integration scaling for the hydrolysis of **2**, **3**, and **4**, because its concentration remained constant throughout. However, this strategy could not be applied in the case of substrate **1**, because the methylene proton signal of the linker arm of **1c** overlaps with the acetate reference. Consequently, in this particular case, the H-6 of 4NTC in the aromatic region, which remains identical in all four 4NTC derivatives, was used for the integration calibration.

Signals usable for hydrolysis monitoring were selected in order to avoid overlapping of products and starting material, as well as being distant enough from the HOD peak as to remain untouched by the solvent signal pre-saturation (Figs. 2–5). As a general rule, the zone between 4.88 and 4.14 ppm could not be exploited since H-2, H-3, H-4, and H-5 protons of the four major different forms of free L-Ara come out in this area. As a result, most protons selected for integration were located in the anomeric region where the H-1 of α-L-Ara*f* is often distinctive enough (Table 1). Hydrolysis of compound **2** was conveniently monitored by following the evolution of the H-6 of 4NTC in the aromatic region, because α-L-Ara*f* substitutions greatly affect its chemical shift. As a result, the starting material, the intermediates, and the final product were all characterized by fairly distinctive signals. The monitoring of the hydrolysis of **3** was more problematic. Firstly, H-1 β-D-Xyl*p* of **3b** overlaps with H-1 of β-L-Ara*p*. Secondly, depending on the reaction temperature, not all signals were always available for integration, as the HOD peak interfered with the Bn methylene signals of **3b** at 303 K. Therefore, the hydrolysis of **3** by AbfB, could only be monitored by measuring the disappearance of the α-L-Ara_B H-1 of **3** (Fig. 4c). Also, the appearance of **3a** in *Ba*AXH-d3 (303 K) experiments was easily tracked through the H-1 β-D-Xyl*p* proton, while its disappearance in AbfA experiments (323 K) was followed with the Bn methylene signal, because of the HOD attenuation shift. Finally, in the case of the natural substrate **4**, all possible intermediates, as well as the final product have already been characterized [19,22,23]. We observed that the signals with the least interference were those of H-2 and H-4 of α-L-Ara_A of **4** when no intermediate was present, which is acceptable in the case reactions involving AbfB and *Tx*Abf, because the formation of intermediates never exceeded 10%. To monitor reactions catalyzed by AbfA and *Ba*AXH-d3, the H-1 of α-L-Ara_B of **4a** was followed, even though a small overlap with the β-L-Ara*f* anomeric signal was observed.

2.6. Evaluation of catalytic activity

Initial rates were derived by analyzing the linear part of the graphs showing the amount of L-Ara*f* units liberated by the enzymes (Fig. 6, and Supplementary Figs. 3–6 and Table 1). Precise intervals between two spectra (data points) were provided by their recording times. For enzymes that are unable to remove both L-Ara*f* moieties from

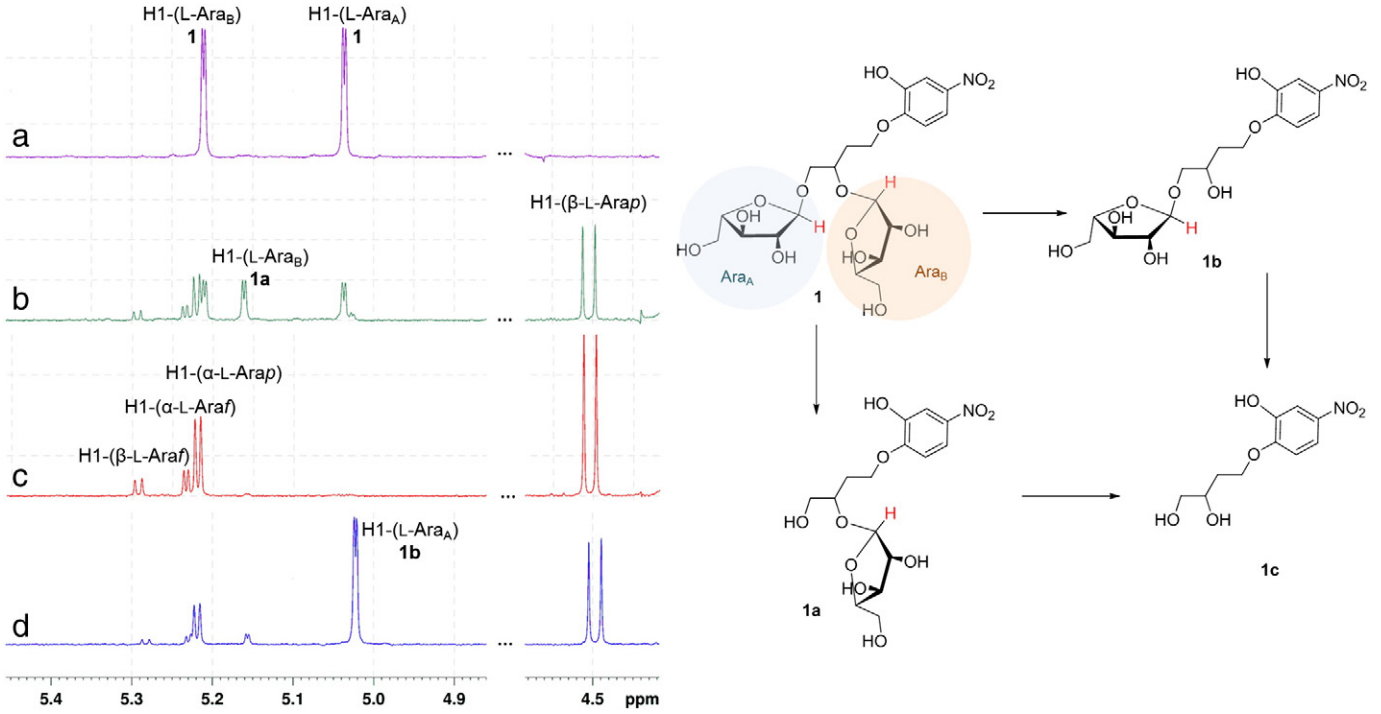

Fig. 2. ^{1}H NMR spectra of the hydrolysis of artificial substrate **1** by different Abfs. a) 5 mM **1** in 20 mM deuterated sodium acetate, pD 5.87; b) after 136 min incubation with *Tx*Abf at 60 °C; c) 296 min incubation with *Tx*Abf at 60 °C; and d) 1074 min incubation with *Ba*AXH-d3 at 30 °C.

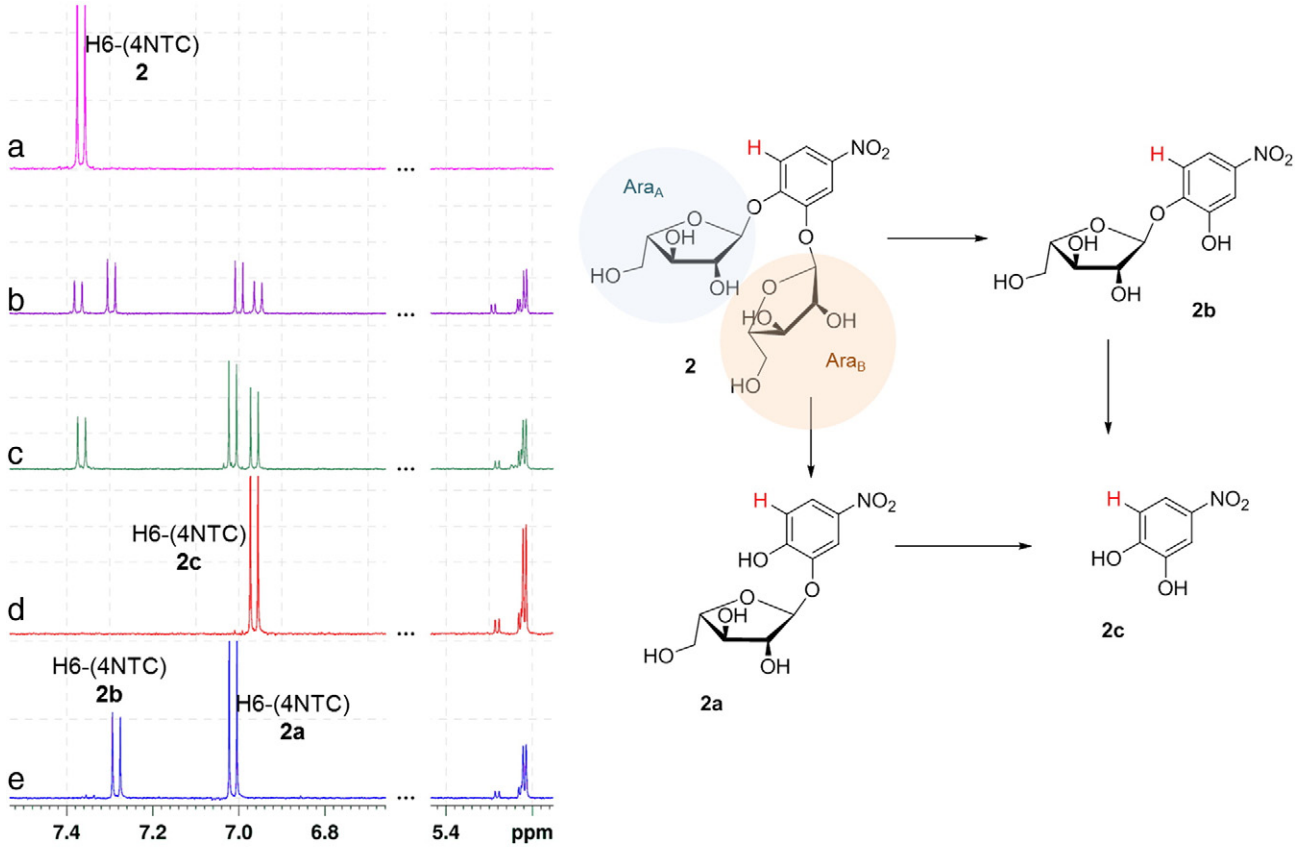

Fig. 3. ^{1}H NMR spectra of the hydrolysis of artificial substrate **2** by different Abfs. a) 5 mM **1** in 20 mM deuterated sodium acetate, pD 5.87; b) after 80 min incubation with *Tx*Abf at 60 °C; c) 105 min incubation with AbfB at 30 °C; d) 437 min incubation with AbfB at 30 °C; and e) 221 min incubation with *Ba*AXH-d3 at 30 °C.

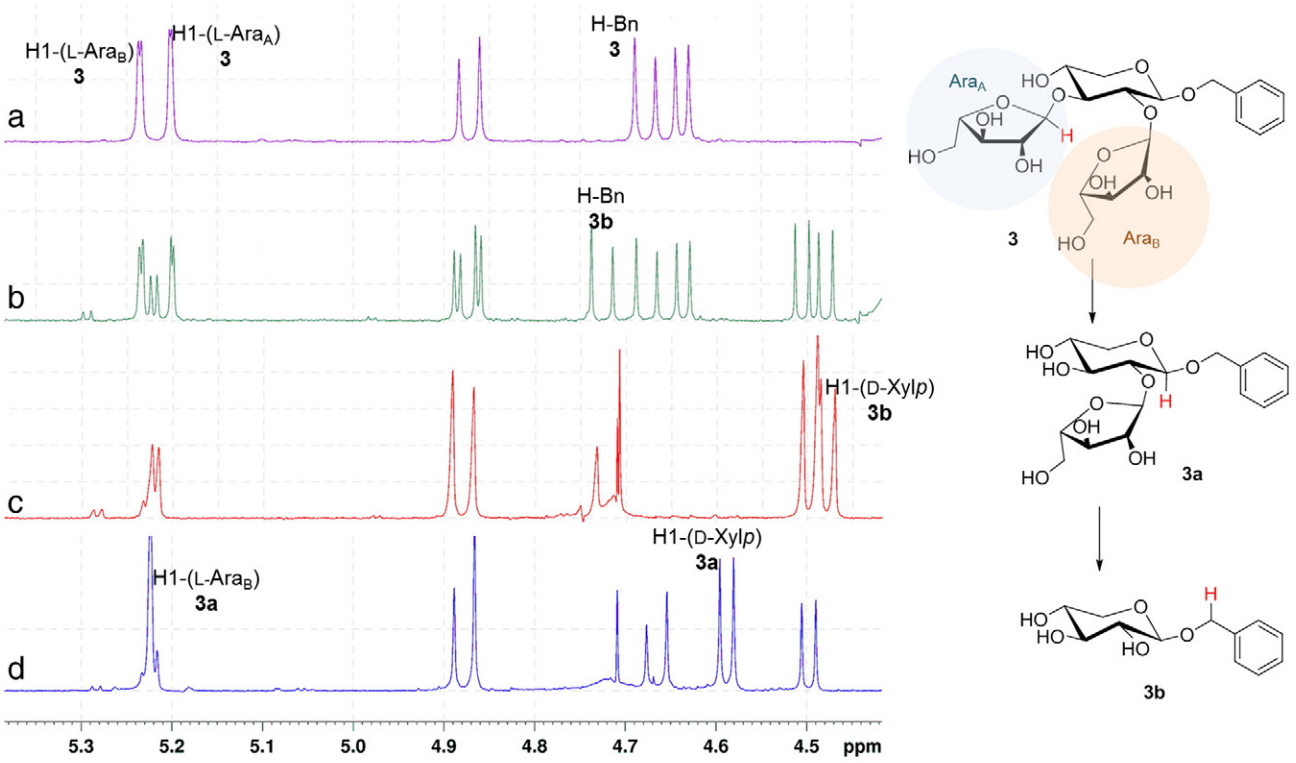

Fig. 4. [1]H NMR spectra of the hydrolysis of pseudo-natural substrate **3** by different Abfs. a) 5 mM **3** in 20 mM deuterated sodium acetate, pD 5.87; b) after 78 min incubation with *Tx*Abf at 60 °C; c) 493 min incubation with AbfB at 30 °C; d) 140 min incubation with *Ba*AXH-d3 at 30 °C.

disubstituted D-Xyl*p* moieties, the total amount of sugar released was inferred from the time-dependent consumption of the starting material, except in the case of *Ba*AXH-d3-catalyzed hydrolysis of **4**, where the appearance of **4a** was monitored instead. In the case of enzymes able to cleave both L-Ara*f* moieties, the total amount of free sugar was calculated based on the consumption of the starting material, as well as the

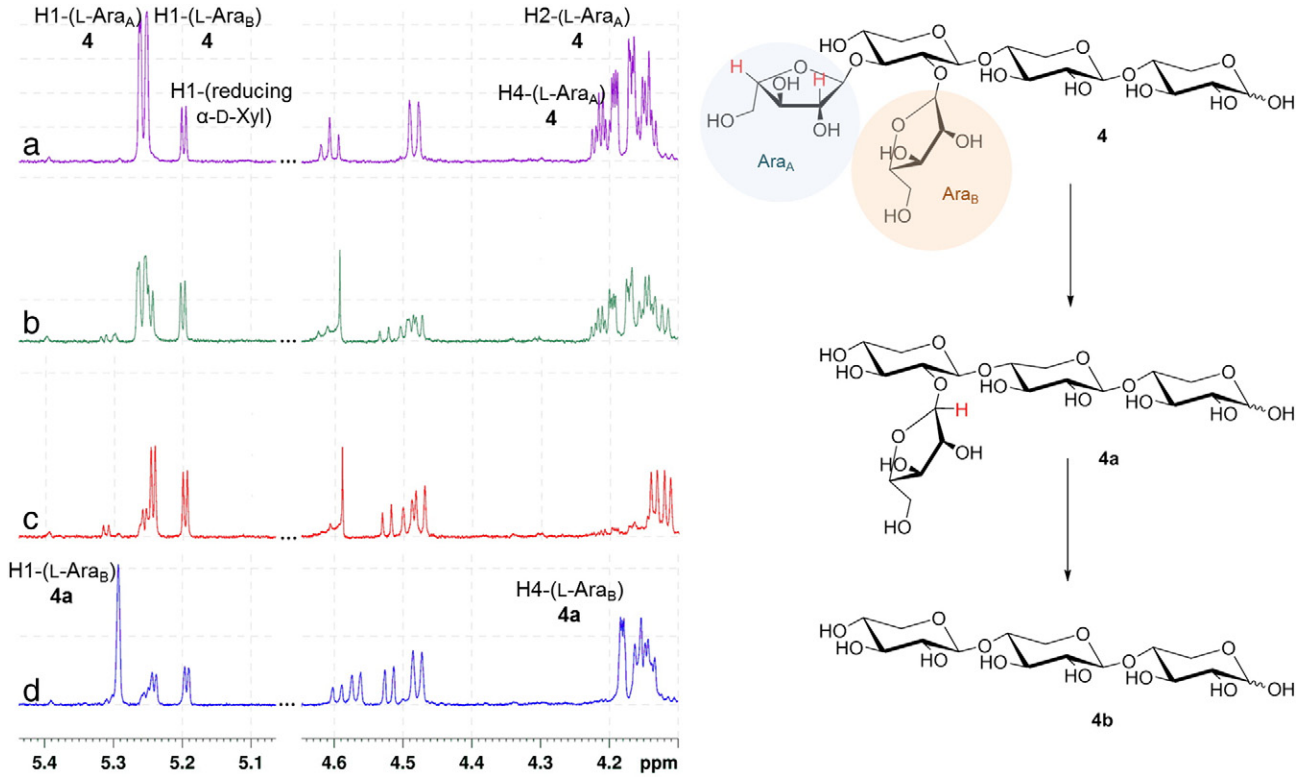

Fig. 5. [1]H NMR spectra of the hydrolysis of natural AXOS **4** by different Abfs. a) 2 mM **4** in 20 mM deuterated sodium acetate, pD 5.87; b) after 82 min incubation with *Tx*Abf at 40 °C; c) 291 min incubation with *Tx*Abf at 40 °C; and d) 39 min incubation with *Ba*AXH-d3 at 30 °C.

Table 1
List of the proton signals used for the tracking of the different species involved during the Abf-catalyzed enzymatic reactions.

Compound	Integrated proton	Signal multiplicity, δ in ppm (J in Hz)	Enzymatic reaction monitoring
β-L-Ara*p*	H1	d, 4.50 (7.8)	AXH-d3(a), AbfB(a), *Tx*Abf(a) with **1** and **3**
α-L-Ara*p*	H1	d, 5.22 (3.6)	*Ba*AXH-d3(a), AbfB(a), *Tx*Abf(a) AbfA(a) with **2**
α-L-Ara*f*	H1	d, 5.23 (2.6)	
β-L-Ara*f*	H1	d, 5.29 (4.7)	
1	H1-(L-Ara_A)	d, 5.04 (1.6)	*Ba*AXH-d3(d), AbfA(d), *Tx*Abf(d), AbfB(d)
1a	H1-(L-Ara_B)	d, 5.16 (1.5)	*Ba*AXH-d3(a), AbfA(d), *Tx*Abf(ad), AbfB(ad)
1b	H1-(L-Ara_A)	d, 5.02 (1.4)	*Ba*AXH-d3(a), AbfA(d), *Tx*Abf(ad), AbfB(ad)
2	H6-(4NTC)	d, 7.37 (9.0)	*Ba*AXH-d3(d), AbfA(d), *Tx*Abf(d), AbfB(d)
2a	H6-(4NTC)	d, 7.01 (9.0)	*Ba*AXH-d3(a), AbfA(d), *Tx*Abf(ad), AbfB(ad)
2b	H6-(4NTC)	d, 7.29 (9.0)	*Ba*AXH-d3(a), AbfA(d), *Tx*Abf(ad)
2c	H6-(4NTC)	d, 6.96 (9.0)	AbfA(a), *Tx*Abf(a), AbfB(a)
3	H1-(L-Ara_A)	d, 5.24 (1.5)	*Ba*AXH-d3(d), AbfB(d), *Tx*Abf(d)
3a	H1-(D-Xyl*p*)	d, 4.59 (7.6)	*Ba*AXH-d3(a)
3a	CH_2 (Bn)	d, 4.68 (11.4)	AbfA(d)
3b	CH_2 (Bn)	d, 4.73 (11.6)	AbfA(a), *Tx*Abf(a)
4	H4 and H2-(L-Ara_A) (A^3)	td, 4.21 (3.4, 1.7) dd, 4.19 (5.7, 3.4)	AbfB(d), *Tx*Abf(d)[a]
4a	H1-(L-Ara_B) (A^2)	s, 5.29	*Ba*AXH-d3(a), AbfA(d)[a], *Tx*Abf(ad)[a], AbfB(ad)

(a): appearance, (d): disappearance.
[a] Hydrolysis of **4** and **4a** mediated by *Tx*Abf and AbfA were done at 313 K due to the cryoprobe temperature limitation.

amount of final product liberated. An accurate measurement of the zero time point was impossible due to the intrinsic limits of the experiment (i.e. the time required to stabilize temperature).

3. Results

To provide a detailed investigation of Abf activity, we focused our attention on the question of how the presence of a doubly-linked L-Ara*f* motif in substrates affects the activity of Abfs from different GH families. To achieve this, we used real-time ^{1}H NMR spectroscopy to monitor enzyme reactions and artificial substrates **1** and **2** [7,15], the pseudo-natural A^{2+} ^{3}Bn **3** and the natural substrate A^{2+} ^{3}XX **4** (Figs. 2–5 and Supplementary Fig. 1). Accordingly, we were able to closely probe the action of four Abfs from families GH43 and 51 that display different hydrolytic behavior on AX [2,6,10,20].

3.1. GH43 AXH-d3 from B. adolescentis

*Ba*AXH-d3 hydrolyzed all four substrates, in each case removing only one L-Ara*f*, while leaving the other one in place (Figs. 2d, 3e, 4d, 5d). This was not due to enzyme inactivation, since the enzyme remained sufficiently active at the end of the reaction to be able to hydrolyze a fresh aliquot of substrate (data not shown). The performance of *Ba*AXH-d3 was comparable on compounds **2**, **3** and **4**, but substrate **1** proved to be more resilient (Fig. 6 and Supplementary Table 1). Concerning reaction regioselectivity, only a slight cleavage preference was observed when using substrate **2**, with a final product ratio (**2a**:**2b**) of 63:37. However, much higher selectivity was observed when using compound **1**, since a final product ratio (**1b**:**1a**) of 94:6 was measured. Finally, reactions involving **3** and **4** (i.e. pseudo-natural and natural di-arabinofuranosylated D-Xyl*p* moieties) were regiospecific, yielding only *O*-2 substituted D-Xyl*p* motifs.

3.2. GH43 AbfA from B. adolescentis

AbfA (at a concentration of 3.8 $\mu g \cdot mL^{-1}$) completely hydrolyzed the mono-substituted intermediate compounds **2a**, **2b**, **3a** and **4a** in less than 7 h (Supplementary Fig. 6) and with hydrolytic activities for these substrates being of the same order of magnitude (Fig. 6 and Supplementary Table 1). Nevertheless, AbfA failed to hydrolyze **1b**, even after 24 h incubation. Regarding the doubly-substituted moiety and in accordance with literature data [6,7,15], compounds **1** and **3** were unaffected, even after incubation at 50 °C for 24 h using a >10-fold higher concentration (47.2 $\mu g \cdot mL^{-1}$) of enzyme, although compound **2**

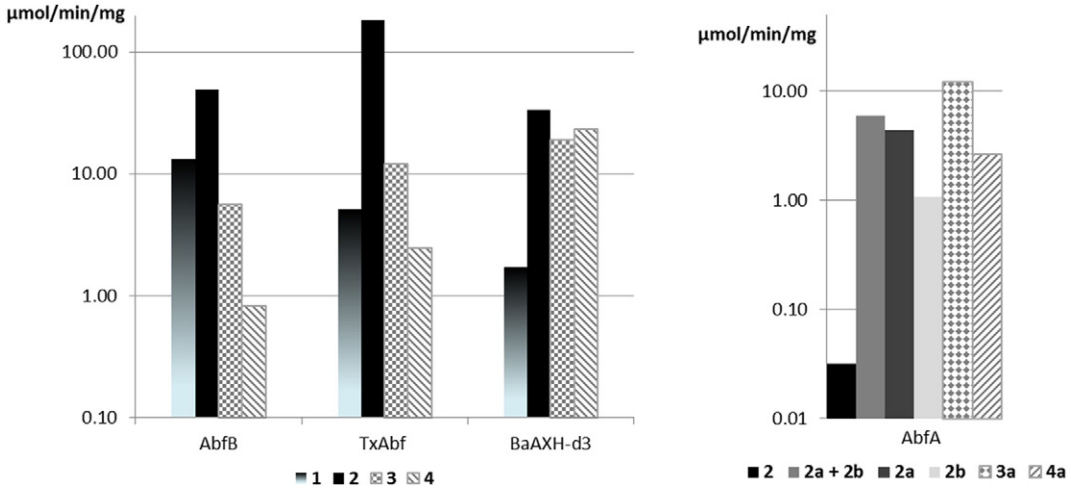

Fig. 6. A logarithmic-scale comparison of the hydrolytic activities of the different Abfs on various di- and mono-arabinofuranosylated substrates. Values refer to the quantity (µmol) of L-Ara unit liberated per min and per mg of enzyme, inferred from the initial rate of the reaction measured by NMR. Since AbfA is inactive towards **1**, **1b**, **3** and **4** and only marginally active on **2**, the activities were measured using a mixture of **2a** and **2b**, **3a** and **4a** generated by the action of *Ba*AXH-d3 on disubstituted moieties.

provided a slightly ambiguous result. Indeed, in identical conditions, 30% of compound **2** were hydrolyzed by AbfA after 24 h, which is 25% higher than the spontaneous hydrolysis that characterized the control reaction. Though measurable, it is noteworthy that the level of hydrolysis observed with **2** was still more than a 100-fold lower than that observed in the AbfA hydrolysis of **2a** and **2b**.

3.3. GH51 Abfs from T. xylanilyticus and B. adolescentis

All of the substrates under study released two units of free L-Ara per unit of initial substrate when digested by *Tx*Abf and AbfB, including natural AXOS **4** (Supplementary Figs. 3 and 4). The efficiency of these enzymes was particularly high with **2** and its mono-glycosylated derivatives (Figs. 6 and 7, and Supplementary Table 1). Mono-glycosylated intermediates were observed during the hydrolysis of **1**, **2** and **4**, but not in **3** (Figs. 2–5). When hydrolyzing **1**, both enzymes preferentially generated **1a**, which attained 31 and 35% mol of the reaction components when using *Tx*Abf and AbfB, respectively, while **1b** never exceeded 5% mol (Figs. 2b–c and 7). Regarding the hydrolysis of **4** by *Tx*Abf or AbfB, the intermediate **4a** (*O*-2 substituted D-Xyl*p* moiety), detectable at 5.29 ppm, reached 10% mol during the reaction, while the characteristic signal of the *O*-3 substituted D-Xyl*p* moiety (5.33 ppm) remained undetectable (Fig. 5b–c). The only major difference in behavior between the two GH51 Abfs concerned their regioselectivity on compound **2** (Fig. 7). In this regard, AbfB only produced **2a**, while *Tx*Abf generated both regioisomers, with a slight preference for **2b**.

4. Discussion

In the present study, we set out to investigate the specificities of different Abfs using a set of substrates. Substrate **1** [15], displays a cleavable linker arm between an unhindered double L-Ara*f* moiety and an aryl leaving group (4NTC), which offers the possibility of free rotation around the bond between the two sugars. This implies that substrate **1** could adopt a *syn*-conformation, although this would not be the favored one. Similarly, substrate **2** bears the 4NTC moiety and the L-Ara*f* units locked in *cis* positions with respect to each other. This substrate was chosen because it has already been demonstrated that it is a good artificial substrate for AXH-d type enzymes [7]. The non-chromogenic substrate **3**, a benzyl di-arabinofuranosylated β-D-xylopyranoside, was included in this study, because it imitates the basic motif of natural disubstituted AXOS structures. The D-Xyl*p* moiety of this compound is locked in β anomery, and is linked to a benzyl (Bn) group that can occupy the subsite +2 in the active site of enzymes. Finally, the terminally L-Ara*f*-disubstituted AXOS, $A^{2+3}XX$ **4** was included, since this is fully representative of a natural L-Ara*f* disubstituted substrate. In **3** and **4**, the L-Ara*f*s are locked in equatorial positions resulting in a small dihedral angle between the two sugars (i.e. corresponding to a *syn* conformation).

4.1. BaAXH-d3, a specialist GH43 enzyme that acts on double-substituted xylan

*Ba*AXH-d3 only released one L-Ara*f* unit from doubly-substituted substrates. This observation is consistent with the known properties of

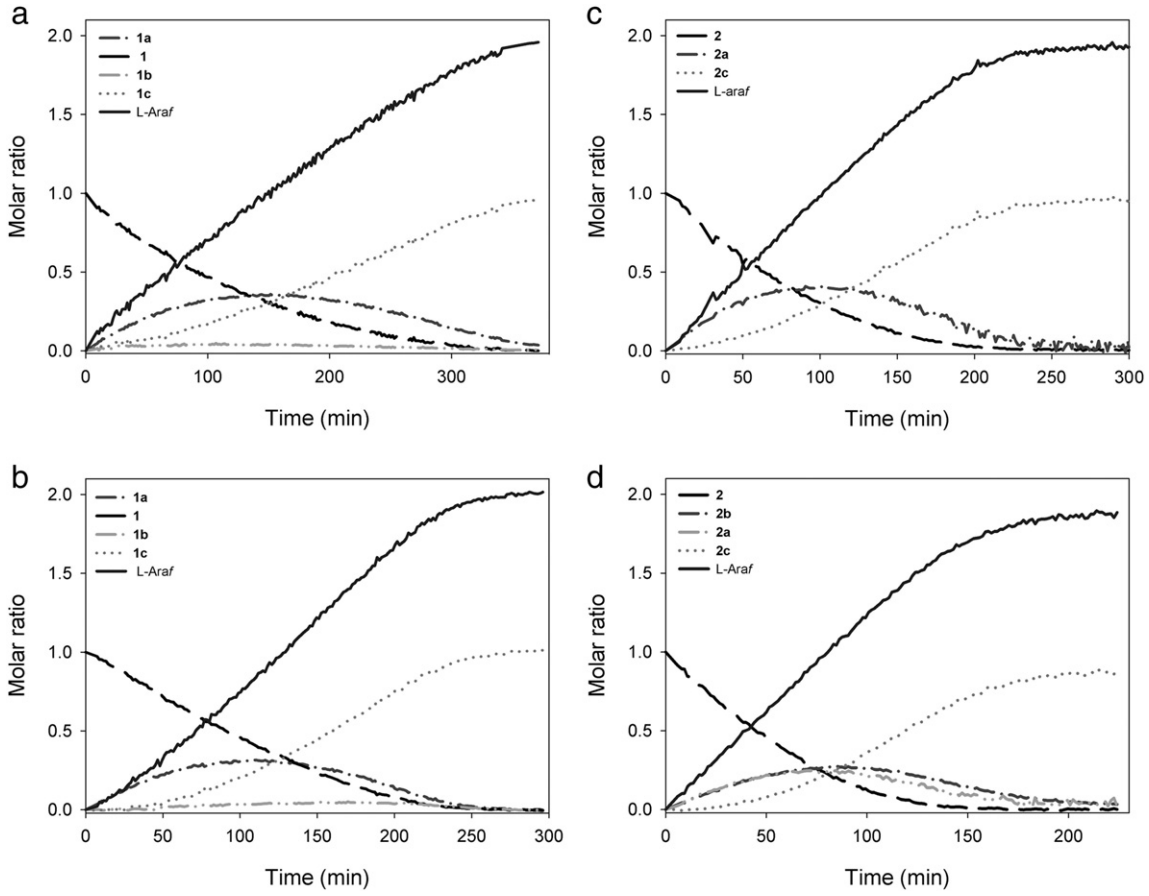

Fig. 7. The time-dependent evolution of relevant (integrated) proton signals during the hydrolysis of artificial substrates, **1** (a and b) and **2** (c and d), by AbfB (a and c) and *Tx*Abf (b and d). The concentrations of fully hydrolyzed product were determined either by measuring the 4NTC moiety signals for the hydrolysis of **2**, or calculated from NMR data for the hydrolysis of **1**. The total free L-Ara was inferred by comparing the substrate and product curves.

this enzyme [6,10] and can be easily explained by considering the probable molecular conformations of the different compounds. In **1** the free rotation across the C – C bond of the chain is likely to lead to preferential positioning of the two sugars in mutual *anti* positions, even though *syn*-positioning (required for enzyme-mediated hydrolysis) remains possible. In practice, in **1** the sugar that is preferentially released is the most hindered one (i.e. the one borne by the secondary hydroxyl group). This suggests that the other sugar, which benefits from a greater degree of freedom, is first to bind to the enzyme, an interaction that is pursued by chain rotation and binding of the hindered sugar into the active site pocket. This explanation is consistent with data from the study of *Hi*AXH-d3 from *H. insolens* that indicates that *Hi*AXH-d3 specifically recognizes the L-Ara*f* unit in the vicinal position of the cleaved sugar [11]. Even if the latter only displays 24% identity with *Ba*AXH-d3, both enzymes nonetheless hold in common eight key active site residues (Supplementary Fig. 7) so the comparison is likely to be valid. In this respect it is also noteworthy that when acting on **3** or **4**, *Ba*AXH-d3 only yielded *O*-2 substituted D-Xyl*p* motifs. Interestingly, this finding contrasts with the data presented for *Hi*AXH-d3 [11], which revealed that this enzyme's strict regioselectivity stems from the interaction of Trp526 with the endocyclic oxygen of the D-Xyl*p* positioned in the +2 subsite, which constitutes the only asymmetric feature of the xylan main-chain. In *Ba*AXH-d3 such an explanation cannot be fully valid, first because there is no equivalent of Trp526 (Supplementary Fig. 7) and second because substrate **3** lacks an endocyclic oxygen in the +2 position. Taken together these observations suggest that the D-Xyl*p* residue in the +1 subsite defines the orientation of the rest of the molecule in the active site. Therefore, in spite of their very similar regiospecific activity on natural disubstituted substrates, our results suggest that the substrate recognition determinants in *Ba*AXH-d3 and *Hi*AXH-d3 are not strictly identical.

4.2. Fine substrate recognition in GH43 AbfA from B. adolescentis

It is known that AbfA specifically releases L-Ara*f* from mono-substituted D-Xyl*p* residues, and is inactive on double-substituted D-Xyl*p* residues [6]. Therefore, the fact that AbfA completely hydrolyzed the mono-substituted species **2a**, **2b**, **3a** and **4a** was expected. However, it was more surprising to find that AbfA cannot hydrolyze **1b**. This rather high selectivity indicates that the +1 subsite of AbfA must possess recognition determinants both for the D-Xyl*p* ring itself and the associated vicinal hydroxyl, because the dissociation of these elements in compound **1b** destroys substrate recognition.

4.3. Family GH51 can completely de-ramify double-substituted D-xylosyl moieties

Apparently, both *Tx*Abf and AbfB display a mixed AXH-m,d activity, since they were able to completely digest the four assayed substrates (Supplementary Figs. 3 and 4). Moreover, the maximum level of production of intermediate reaction products was more dependent on the nature of the substrates than on the enzyme used, suggesting that the activity of both GH51 enzymes is sensitive to structural changes in the vicinity of the scissile bond. For example, when acting on **3** (Fig. 4b–c), neither enzyme produced detectable amount of intermediates, which suggests that the rate-limiting reaction was the first one, required to generate the intermediate compounds. When *Tx*Abf and AbfB hydrolyzed **1**, the preferential production of **1a** was almost certainly a witness to the previously mentioned fact that the L-Ara*f* unit linked to the secondary alcohol group is more hindered than the second L-Ara*f* unit (Figs. 2b–c and 7). Similarly, the fact that both enzymes failed to produce an *O*-3 substituted D-Xyl*p*-containing intermediate compound when hydrolyzing **4** can also be explained by the relative accessibility of the two L-Ara*f* moieties and thus the preference of the enzymes for the 1,3-linked L-Ara*f* moiety, a preference that has already been described for a barley arabinofuranosidase [13]. Moreover, it is noteworthy that the positioning of *O*-3-linked L-Ara*f* unit within −1 subsite is no doubt facilitated in the case of **4**, where the disubstituted D-Xyl*p* moiety is located at the non-reducing terminal. Internal disubstituted D-Xyl*p* moieties are likely to be much more constrained, which explains previous observations, indicating that GH51 Abfs do not generally release L-arabinose from di-arabinofuranosylated D-Xyl*p* moieties in heteroxylans [24]. Moreover, this appears rather logical, since if the *O*-3 L-Ara*f* unit of **4** does indeed bind in the −1 subsite, then it is probable that the *O*-2 L-Ara*f* moiety is bound in subsite +2′, a subsite that accommodates D-Xyl*p* moieties when the GH51 Abfs act on internal L-Ara*f* units. The only major difference in behavior between the two GH51 Abfs involves the regioselectivity associated with the hydrolysis of compound **2**, which suggests that the nitro group can generate a strong interaction that specifically influences the hydrolysis pattern in AbfB (Figs. 3b–d and 7). Nevertheless, the formation of up to 53 and 41% mol of intermediates by *Tx*Abf and AbfB respectively indicates that the recognition of double and mono-substituted species are of the same order of magnitude in both cases. Moreover, it is noteworthy that both enzymes hydrolyzed **2**, **2a** and **2b** more efficiently than the other three compounds (Fig. 6), suggesting that these enzymes show preference for a direct linkage to the aryl leaving group [25]. Indeed, the measured specific activities were consistent with those measured using pNPA [7], inferring that the +1 subsites of these enzymes display strong recognition of the aromatic ring. According to a previous structural analysis [5], the +1 subsite of *Tx*Abf is characterized by the presence of Trp302 and, to a lesser extent, Trp248, which are ideally placed to interact with a sugar ring or an aromatic group, such as 4NTC or pNP. In AbfB it is more difficult to pinpoint the residues that might favor the recognition of aromatic groups in its +1 subsite, but assuming that the catalytic residues are localized at positions 358 and 445 (acid/base and nucleophile) respectively, then one might assume that Trp449 in AbfB is the functional homologue of Trp302 in *Tx*Abf (Supplementary Fig. 8).

Finally, it is noteworthy that the +2′ subsite is partly defined by the amino acid pair His98–Trp99, which is borne on the mobile β2α2 loop [26]. Previously it was suggested that substrate binding in the active site of *Tx*Abf involves an induced fit mechanism and that the movement of the β2α2 loop is only possible because of the presence of a shortened β7α7 loop, which is not a universal feature in family GH51. In AbfB, it is likely that a similar configuration prevails, with Leu263–Trp264 forming part of the β2α2 loop, and associated with a short β7α7 loop. Overall, these observations reinforce the idea that AbfB might also fix substrates using an induced fit mechanism and that both enzymes possess a similar ability to bind terminally-double substituted D-Xyl*p* using the presence of the +1 (D-Xyl*p* binding) and +2′ subsites (L-Ara*f* binding), respectively.

5. Conclusions

Using well-designed artificial substrates we have demonstrated how these can be used to investigate selectivity in Abfs, a property that often remains unstudied due to the lack of appropriate substrates and readily accessible methods. On the basis of our work, we believe that the two chromogenic substrates (**1** and **2**) described here are a useful addition for the discovery and preliminary characterization of Abfs. Beyond this methodological contribution, our work has also revealed several interesting results, but the most important of these is that GH51 Abfs, enzymes that are generally considered to be active on the L-Ara*f* group of mono-substituted D-Xyl*p* in heteroxylans, are also perfectly able to completely debranch di-arabinofuranosylated D-Xyl*p* moieties, when these are located at the non-reducing end of xylo-oligosaccharides and probably heteroxylans. In the context of AX degradation by complex enzyme consortia this observation is significant, because it is likely that xylo-oligosaccharides bearing a non-reducing di-arabinofuranosylated D-Xyl*p* moiety are a quite frequent occurrence, being a possible product of GH10 xylanase-mediated hydrolysis [27].

Acknowledgements

This work was supported by Région Midi-Pyrénées grant DAER Recherche 10008500 (to V.B.). MetaToul (Metabolomics & Fluxomics Facitilies, Toulouse, France, www.metatoul.fr) and its staff members (Lindsay Peyriga, Edern Cahoreau and Jean-Charles Portais) are gratefully acknowledged for the technical support and access to NMR facility. MetaToul is part of the national infrastructure MetaboHUB (The French National infrastructure for metabolomics and fluxomics, www.metabohub.fr). MetaToul is supported by grants from the Région Midi-Pyrénées, the European Regional Development Fund, the SICOVAL, the Infrastructures en Biologie Sante et Agronomie (IBiSa, France), the Centre National de la Recherche Scientifique (CNRS) and the Institut National de la Recherche Agronomique (INRA). NMR experiments were also performed on the PICT — Genotoul platform of Toulouse and funded by CNRS, Université de Toulouse—UPS, IBiSa, European structural funds and the Midi-Pyrénées region.

Appendix A. Supplementary Data

Supplementary data to this article can be found online at http://dx.doi.org/10.1016/j.bbagen.2014.07.001.

References

[1] C. Dumon, L. Song, S. Bozonnet, R. Fauré, M.J. O'Donohue, Progress and future prospects for pentose-specific biocatalysts in biorefining, Process Biochem. 47 (2012) 346–357.
[2] S. Lagaert, A. Pollet, C.M. Courtin, G. Volckaert, β-Xylosidases and α-L-arabinofuranosidases: accessory enzymes for arabinoxylan degradation, Biotechnol. Adv. 32 (2014) 316–332.
[3] V. Lombard, H. Golaconda Ramulu, E. Drula, P.M. Coutinho, B. Henrissat, The carbohydrate-active enzymes database (CAZy) in 2013, Nucleic Acids Res. 42 (2014) D490–D495.
[4] K. Hövel, D. Shallom, K. Niefind, V. Belakhov, G. Shoham, T. Baasov, Y. Shoham, D. Schomburg, Crystal structure and snapshots along the reaction pathway of a family 51 α-L-arabinofuranosidase, EMBO J. 22 (2003) 4922–4932.
[5] G. Paës, L.K. Skov, M.J. O'Donohue, C. Rémond, J.S. Kastrup, M. Gajhede, O. Mirza, The structure of the complex between a branched pentasaccharide and *Thermobacillus xylanilyticus* GH-51 arabinofuranosidase reveals xylan-binding determinants and induced fit, Biochemistry 47 (2008) 7441–7451.
[6] S. Lagaert, A. Pollet, J.A. Delcour, R. Lavigne, C.M. Courtin, G. Volckaert, Substrate specificity of three recombinant α-L-arabinofuranosidases from *Bifidobacterium adolescentis* and their divergent action on arabinoxylan and arabinoxylan oligosaccharides, Biochem. Biophys. Res. Commun. 402 (2010) 644–650.
[7] V. Borsenberger, F. Ferreira, A. Pollet, E. Dornez, M.-L. Desrousseaux, S. Massou, C.M. Courtin, M.J. O'Donohue, R. Fauré, A versatile and colorful screening tool for the identification of arabinofuranose-acting enzymes, ChemBioChem 13 (2012) 1885–1888.
[8] H.R. Sørensen, C.T. Jørgensen, C.H. Hansen, C.I. Jørgensen, S. Pedersen, A.S. Meyer, A novel GH43 α-L-arabinofuranosidase from *Humicola insolens*: mode of action and synergy with GH51 α-L-arabinofuranosidases on wheat arabinoxylan, Appl. Microbiol. Biotechnol. 73 (2006) 850–861.
[9] L. Pouvreau, R. Joosten, S.W.A. Hinz, H. Gruppen, H.A. Schols, *Chrysosporium lucknowense* C1 arabinofuranosidases are selective in releasing arabinose from either single or double substituted xylose residues in arabinoxylans, Enzym. Microb. Technol. 48 (2011) 397–403.
[10] K.M.J. Van Laere, G. Beldman, A.G.J. Voragen, A new arabinofuranohydrolase from *Bifidobacterium adolescentis* able to remove arabinosyl residues from double-substituted xylose units in arabinoxylan, Appl. Microbiol. Biotechnol. 47 (1997) 231–235.
[11] L.S. McKee, M.J. Peña, A. Rogowski, A. Jackson, R.J. Lewis, W.S. York, K.B.R.M. Krogh, A. Viksø-Nielsen, M. Skjøt, H.J. Gilbert, J. Marles-Wright, Introducing endo-xylanase activity into an exo-acting arabinofuranosidase that targets side chains, Proc. Natl. Acad. Sci. U. S. A. 109 (2012) 6537–6542.
[12] M.-H. Beylot, V.A. McKie, A.G.J. Voragen, C.H.L. Doeswijk-Voragen, H.J. Gilbert, The *Pseudomonas cellulosa* glycoside hydrolase familly 51 arabinofuranosidase exhibits wide substrate specificity, Biochem. J. 358 (2001) 607–614.
[13] H. Ferré, A. Broberg, J.O. Duus, K.K. Thomsen, A novel type of arabinoxylan arabinofuranohydrolase isolated from germinated barley. Analysis of substrate preference and specificity by nano-probe NMR, Eur. J. Biochem. 267 (2000) 6633–6641.
[14] R.C. Lee, R.A. Burton, M. Hrmova, G.B. Fincher, Barley arabinoxylan arabinofuranohydrolases: purification, characterization and determination of primary structures from cDNA clones, Biochem. J. 356 (2001) 181–189.
[15] V. Borsenberger, E. Dornez, M.-L. Desrousseaux, C.M. Courtin, M.J. O'Donohue, R. Fauré, A substrate for the detection of broad specificity α-L-arabinofuranosidases with indirect release of a chromogenic group, Tetrahedron Lett. 54 (2013) 3063–3066.
[16] E.V. Evtushenko, Regioselective benzoylation of glycopyranosides by benzoic anhydride in the presence of $Cu(CF_3COO)_2$, Carbohydr. Res. 359 (2012) 111–119.
[17] Y. Du, Q. Pan, F. Kong, An efficient and concise regioselective synthesis of α-(1→5)-linked L-arabinofuranosyl oligosaccharides, Carbohydr. Res. 329 (2000) 17–24.
[18] R. Fauré, C.M. Courtin, J.A. Delcour, C. Dumon, C.B. Faulds, G.B. Fincher, S. Fort, S.C. Fry, S. Halila, M.A. Kabel, L. Pouvreau, B. Quemener, A. Rivet, L. Saulnier, H.A. Schols, H. Driguez, M.J. O'Donohue, A brief and informationally rich naming system for oligosaccharide motifs of heteroxylans found in plant cell walls, Aust. J. Chem. 62 (2009) 533–537.
[19] H. Pastell, P. Tuomainen, L. Virkki, M. Tenkanen, Step-wise enzymatic preparation and structural characterization of singly and doubly substituted arabinoxylo-oligosaccharides with non-reducing end terminal branches, Carbohydr. Res. 343 (2008) 3049–3057.
[20] T. Debeche, N. Cummings, I. Connerton, P. Debeire, M.J. O'Donohue, Genetic and biochemical characterization of a highly thermostable α-L-arabinofuranosidase from *Thermobacillus xylanilyticus*, Appl. Environ. Microbiol. 66 (2000) 1734–1736.
[21] P.K. Glasoe, F.A. Long, Use of glass electrode to mesure acidities in deuterium oxide, J. Phys. Chem. 64 (1960) 188–190.
[22] R.A. Hoffmann, B.R. Leeflang, M.M.J. de Barse, J.P. Kamerling, J.F.G. Vliegenthart, Characterisation by ^{1}H-n.m.r. spectroscopy of oligosaccharides, derived from arabinoxylans of white endosperm of wheat, that contain the elements →4)[α-L-Ara*f*-(1→3)]-β-D-Xyl*p*-(1→ or →4)[α-L-Ara*f*-(1→2)][α-L-Ara*f*-(1→3)]-β-D-Xyl*p*-(1→, Carbohydr. Res. 221 (1991) 63–81.
[23] H. Gruppen, R.A. Hoffmann, F.J.M. Kormelink, A.G.J. Voragen, J.P. Kamerling, J.F.G. Vliegenthart, Characterisation by ^{1}H NMR spectroscopy of enzymically derived oligosaccharides from alkali-extractable wheat-flour arabinoxylan, Carbohydr. Res. 233 (1992) 45–64.
[24] C. Rémond, I. Boukari, G. Chambat, M. O'Donohue, Action of a GH 51 α-L-arabinofuranosidase on wheat-derived arabinoxylans and arabinoxylooligosaccharides, Carbohydr. Polym. 72 (2008) 424–430.
[25] L. Novaroli, G. Bouchard Doulakas, M. Reist, B. Rolando, R. Fruttero, A. Gasco, P.-A. Carrupt, The lipophilicity behavior of three catechol-O-methyltransferase (COMT) inhibitors and simple analogues, Helv. Chim. Acta 89 (2006) 144–152.
[26] F. Arab-Jaziri, B. Bissaro, S. Barbe, O. Saurel, H. Débat, C. Dumon, V. Gervais, A. Milon, I. André, R. Fauré, M.J. O'Donohue, Functional roles of H98 and W99 and β2α2 loop dynamics in the α-L-arabinofuranosidase from *Thermobacillus xylanilyticus*, FEBS J. 279 (2012) 3598–3611.
[27] G. Pell, E.J. Taylor, T.M. Gloster, J.P. Turkenburg, C.M.G.A. Fontes, L.M.A. Ferreira, T. Nagy, S.J. Clark, G.J. Davies, H.J. Gilbert, The mechanisms by which family 10 glycoside hydrolases bind decorated substrates, J. Biol. Chem. 279 (2004) 9597–9605.